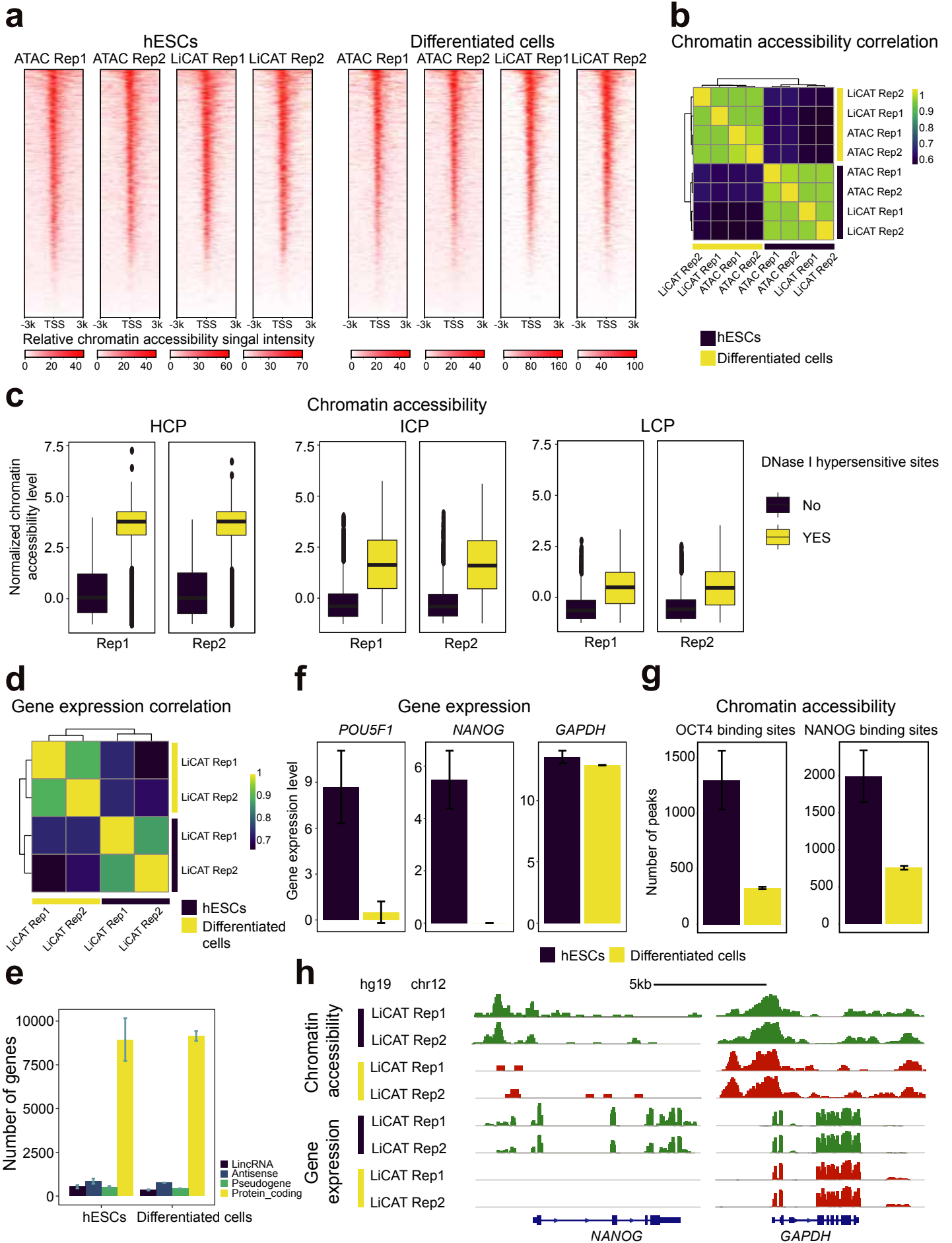
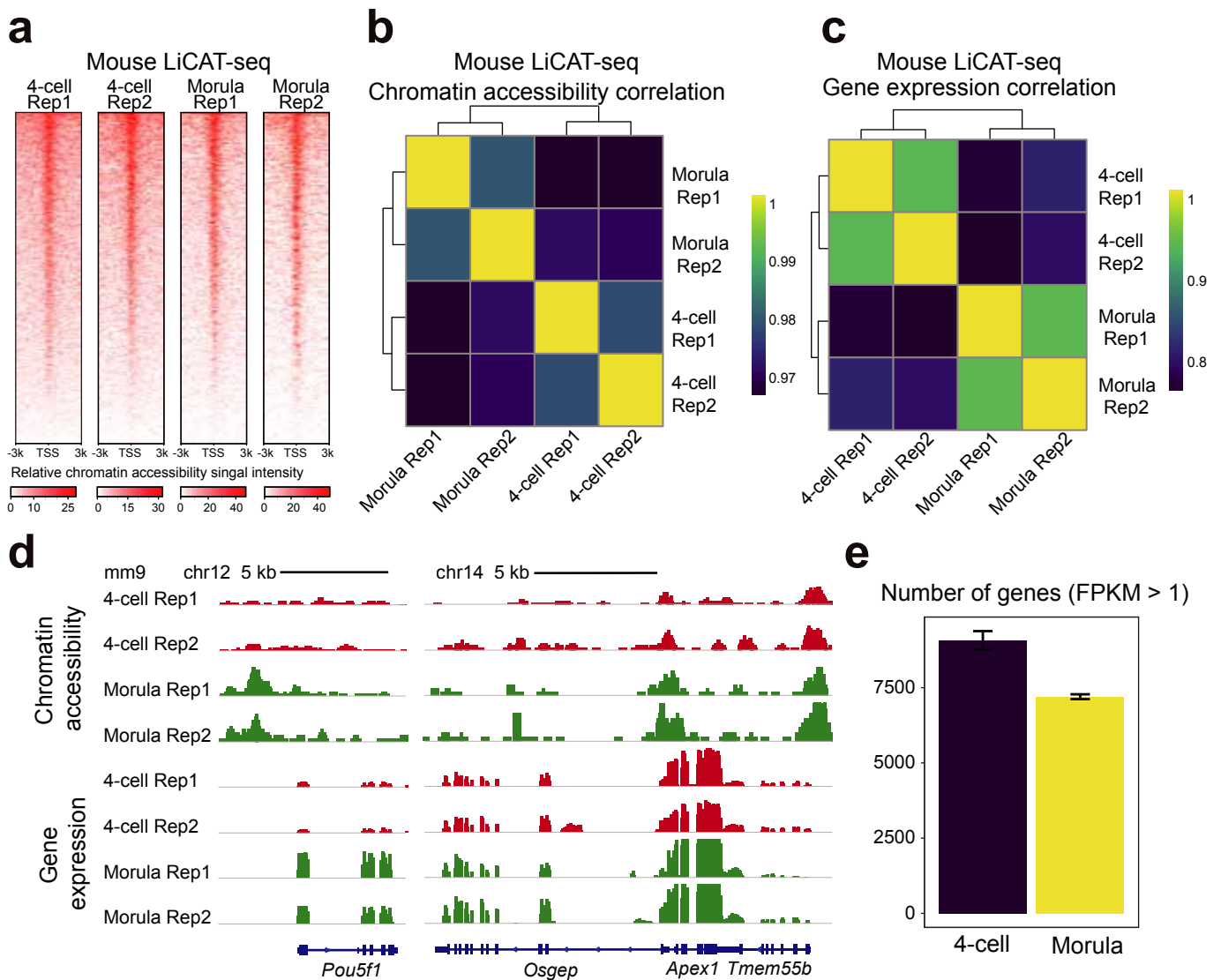


**An integrated chromatin accessibility and transcriptome  
landscape of human pre-implantation embryos**

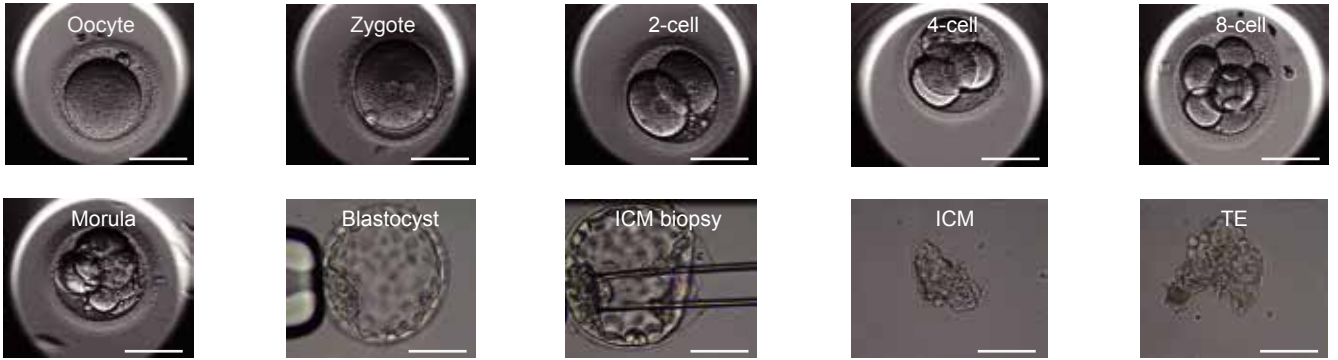
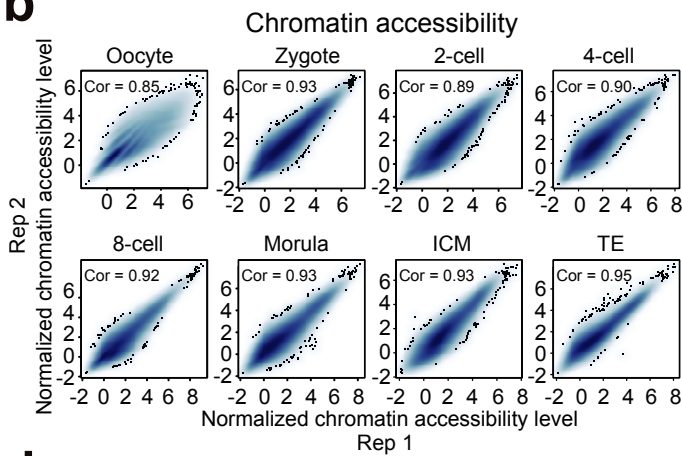
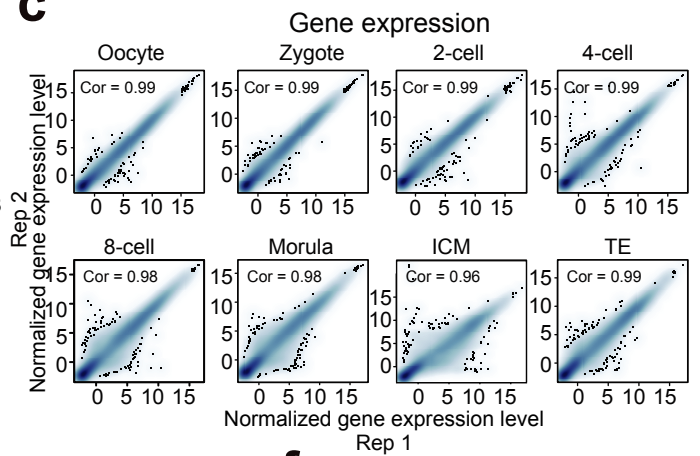
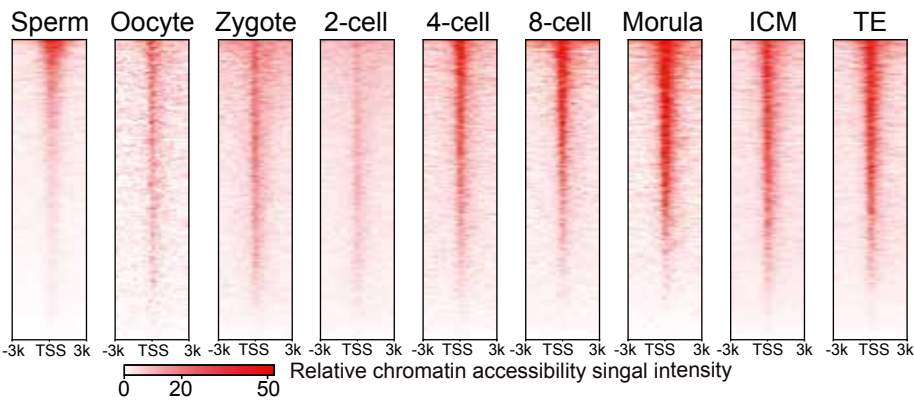
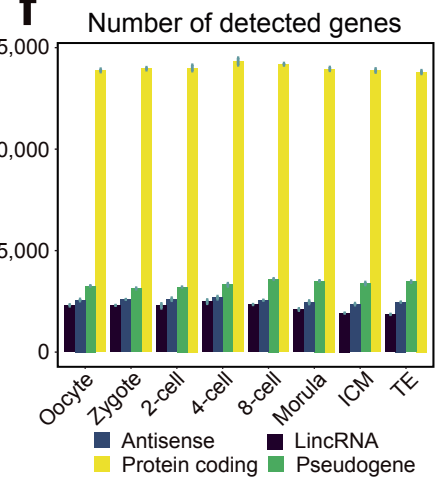
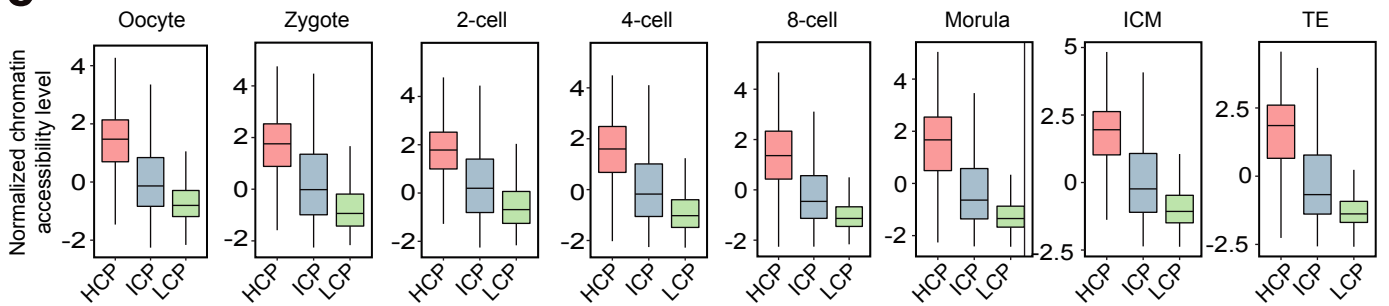
**Liu *et al.***



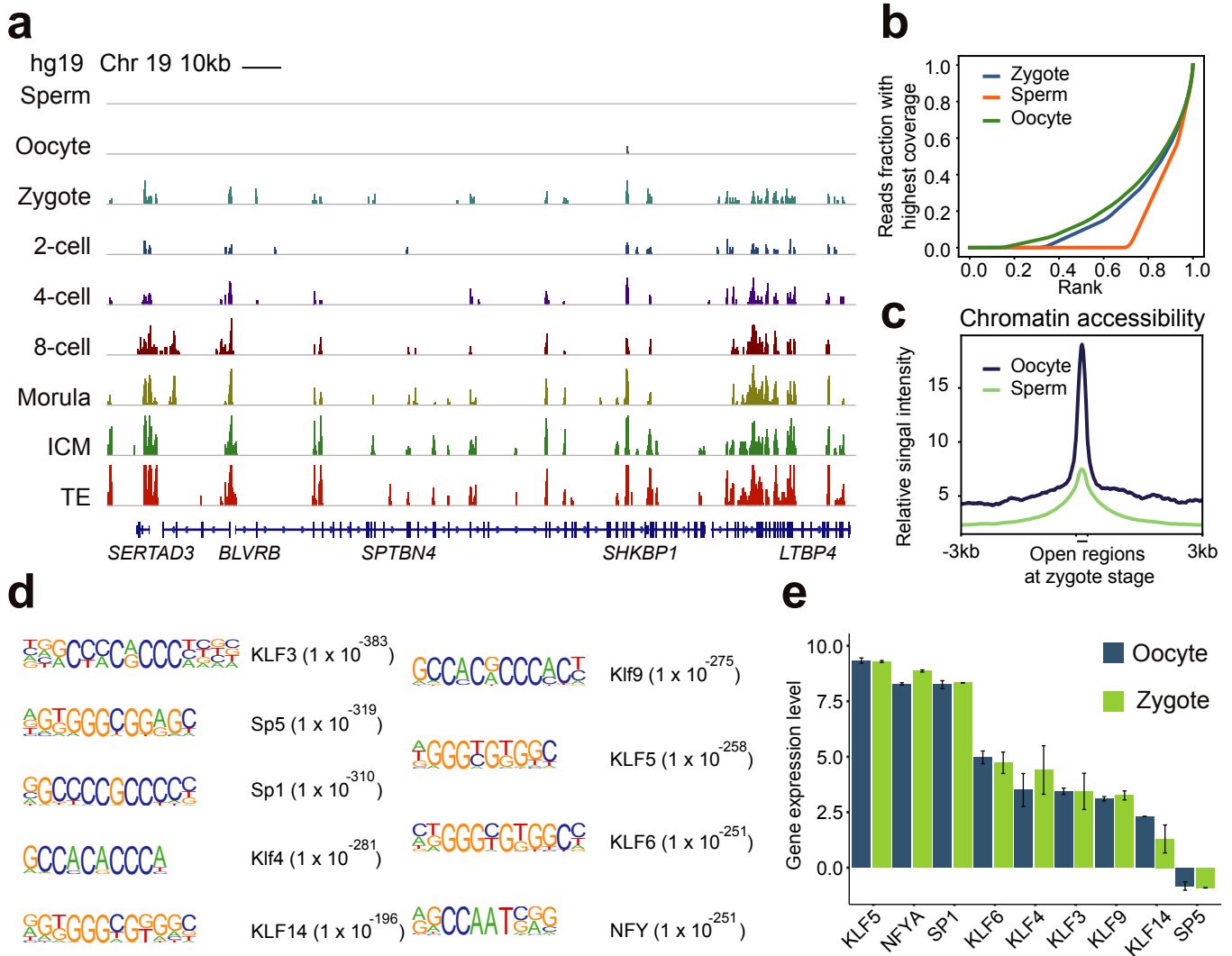
**Supplementary Figure 1: Quality evaluation of LiCAT-seq generated chromatin accessibility and gene expression datasets from hESCs and differentiated cells.** (a) Heat maps showing the enrichment of chromatin accessibility reads around TSSs in LiCAT-seq profiles generated from 10 cells and ATAC-seq profiles generated from 50,000 cells. (b) Pearson correlations between the indicated chromatin accessibility profiles. (c) The chromatin accessibility signal density on the HCPs, ICPs and LCPs at the indicated stages. The HCPs, ICPs and LCPs are divided into two groups based on their DNase I hypersensitivity. The DNase I hypersensitive site dataset was downloaded from AnnotationHub (ID: AH22507). (d) Pearson correlations between the indicated gene expression profiles. (e) Number of genes detected in LiCAT-seq profiles of 4-cell and morula stages of mouse embryo development. (f) Number of chromatin accessibility peaks on NANOG and OCT4 binding sites in hESCs and differentiated cells. The NANOG and OCT4 binding sites in hESCs were downloaded from AnnotationHub (NANOG ID: AH22662; OCT4 ID: AH22667). (g) The expression level of *NANOG*, *OCT4* and *GAPDH* in hESCs and differentiated cells. (h) Genome browser views showing the chromatin accessibility and gene expression signal around *NANOG* and *GAPDH* genes. The error bars shown in this figure represent the mean  $\pm$  standard deviation (SD) of two replicates.



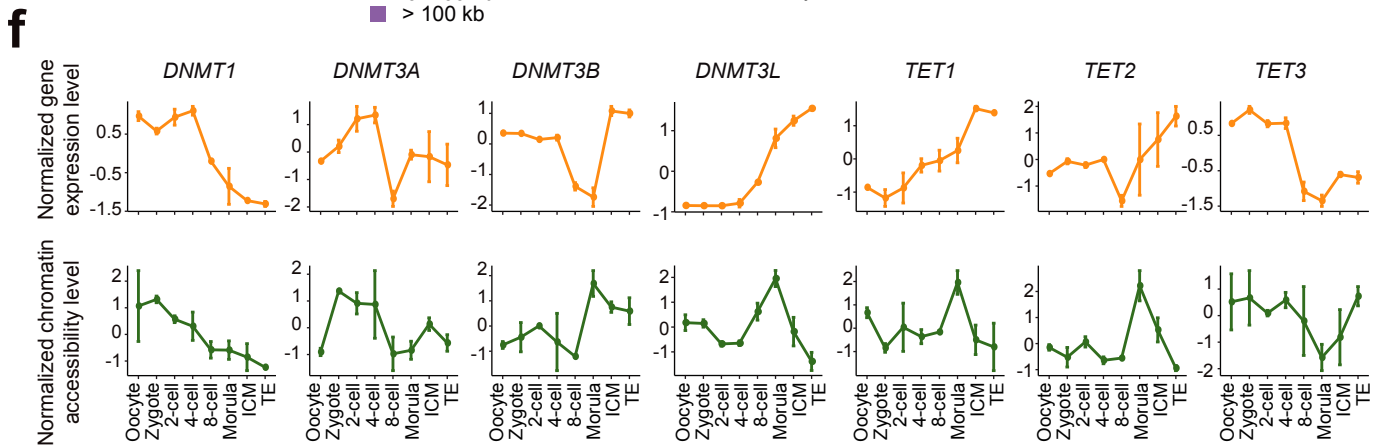
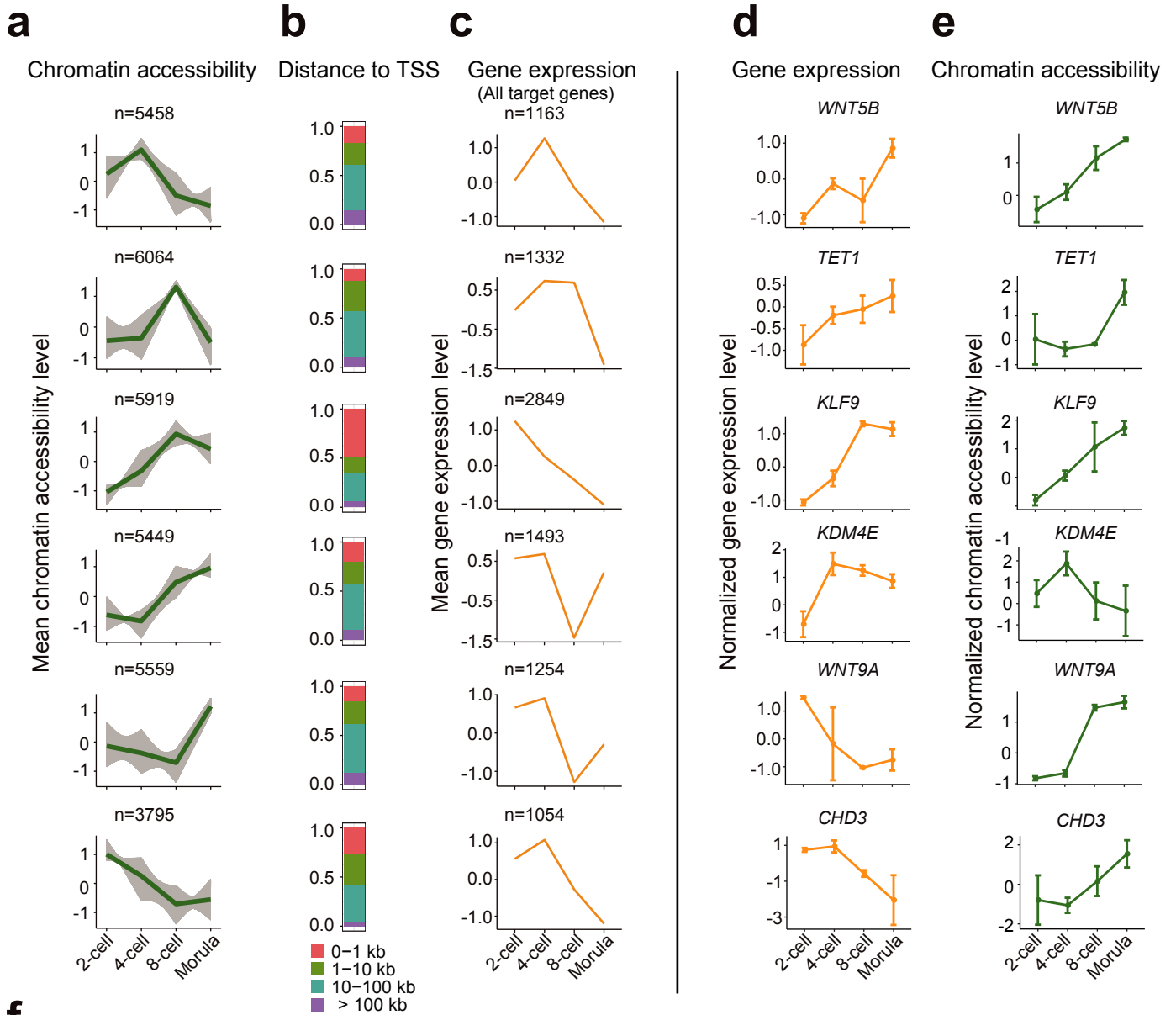
**Supplementary Figure 2: Quality evaluation of LiCAT-seq generated chromatin accessibility and gene expression datasets from mouse embryos. (a)** Heat maps showing the enrichment of chromatin accessibility reads around TSSs in LiCAT-seq profiles generated from 4-cell and morula stages of mouse embryo development. **(b)** Pearson correlations between the indicated chromatin accessibility profiles. **(c)** Pearson correlations between the indicated gene expression profiles. **(d)** Genome browser views showing the chromatin accessibility and gene expression signal around *Oct4* and *Osgep* genes. **(e)** Number of genes detected in LiCAT-seq profiles of 4-cell and morula stages of mouse embryo development. The error bars shown in this figure represent the mean  $\pm$  standard deviation (SD) of two replicates.

**a****b****c****d****f****e**

**Supplementary Figure 3: Quality assessment of chromatin accessibility and gene expression profiles of human preimplantation embryos.** **(a)** Microscopy imaging of mature human oocytes and preimplantation embryos at the zygote, 2-cell, 4-cell, 8-cell, morula and blastocyst stages (isolated inner cell mass (ICM) and trophectoderm (TE) cells). The scale bars on images of Oocyte, Zygote, 2-cell, 4-cell, 8-cell, Morula, Blastocyst and ICM biopsy represent 50  $\mu\text{m}$ ; The scale bars on images of ICM and TE represent 100  $\mu\text{m}$ . **(b)** and **(c)** Scatterplots showing high correlation of chromatin accessibility **(b)** and gene expression **(c)** levels between the two biological replicates of LiCAT-seq profiles at the indicated stages. **(d)** Heat maps showing the enrichment of chromatin accessibility reads around TSSs in each developmental stage. **(e)** The chromatin accessibility signal density on the HCPs, ICPs and LCPs at the indicated stages. **(f)** Number of genes detected at the indicated stages. The error bars shown in this figure represent the mean  $\pm$  standard deviation (SD) of two replicates.

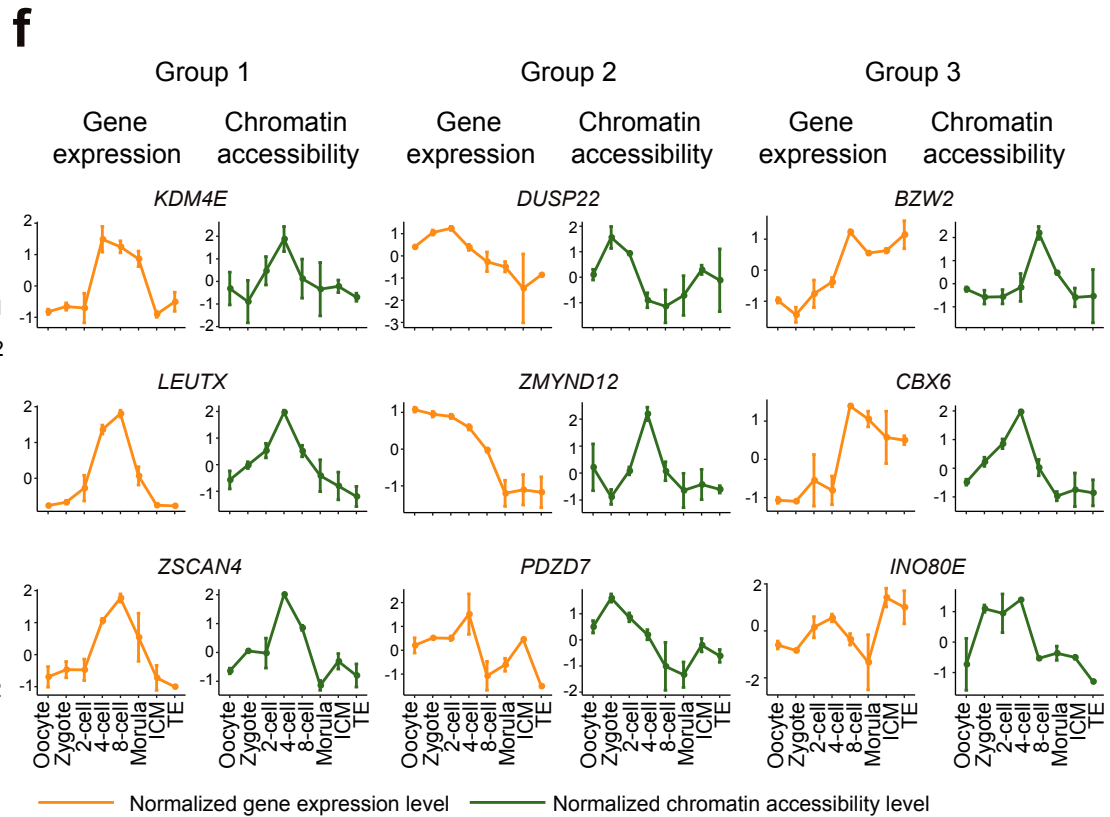
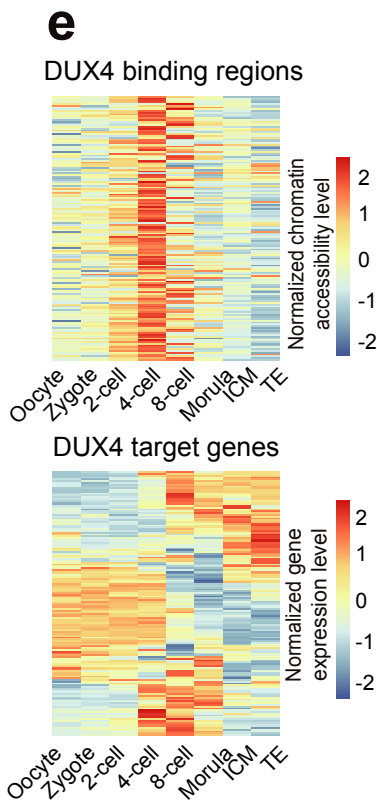
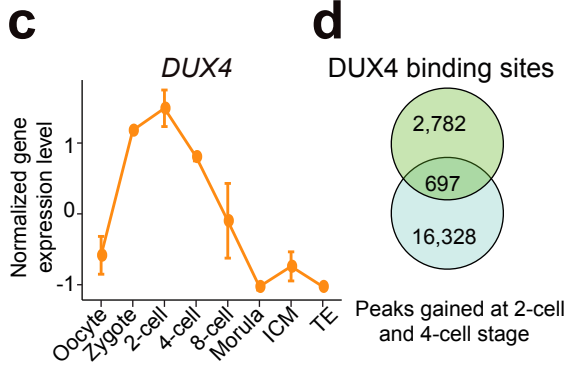
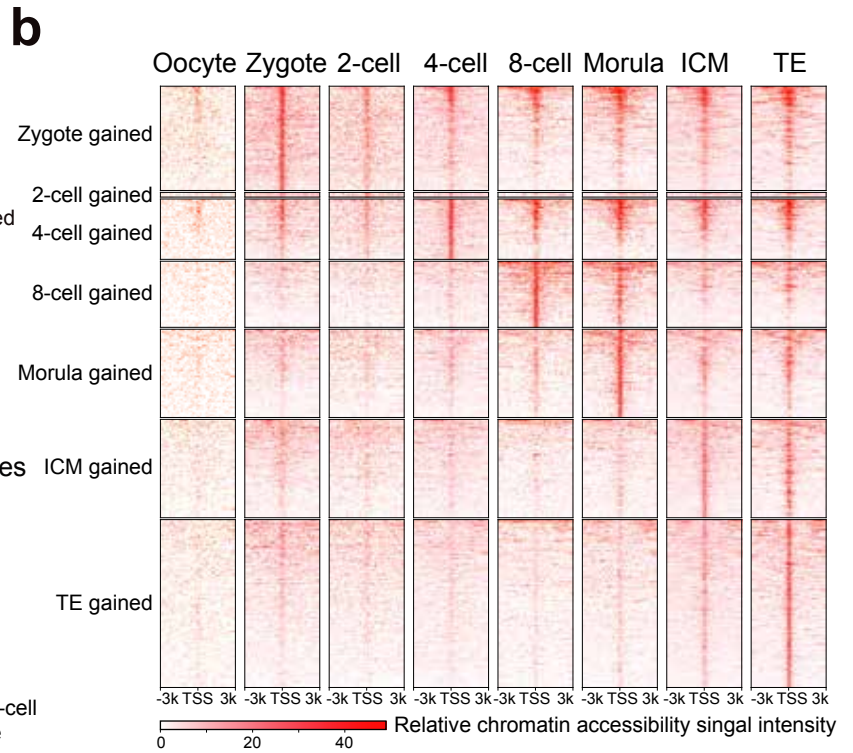
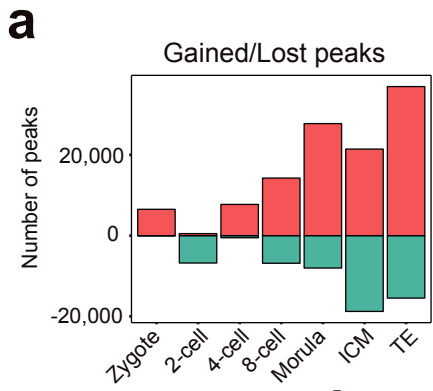


**Supplementary Figure 4: Unique chromatin accessibility features at zygote stage. (a)** Genome browser view showing the chromatin accessibility peaks within a constitutive accessible region. **(b)** Cumulative sum of regions with different ranks of sequencing coverage showing the enrichment of chromatin accessibility read in specific regions. **(c)** Relative read density around open regions of the zygote stage. **(d)** Enrichment of the indicated transcription factor motifs found within open regions of the zygote stage. **(e)** Expression level of the indicated TFs (shown in **d**) in the oocyte. The error bars shown in this figure represent the mean  $\pm$  standard deviation (SD) of two replicates.

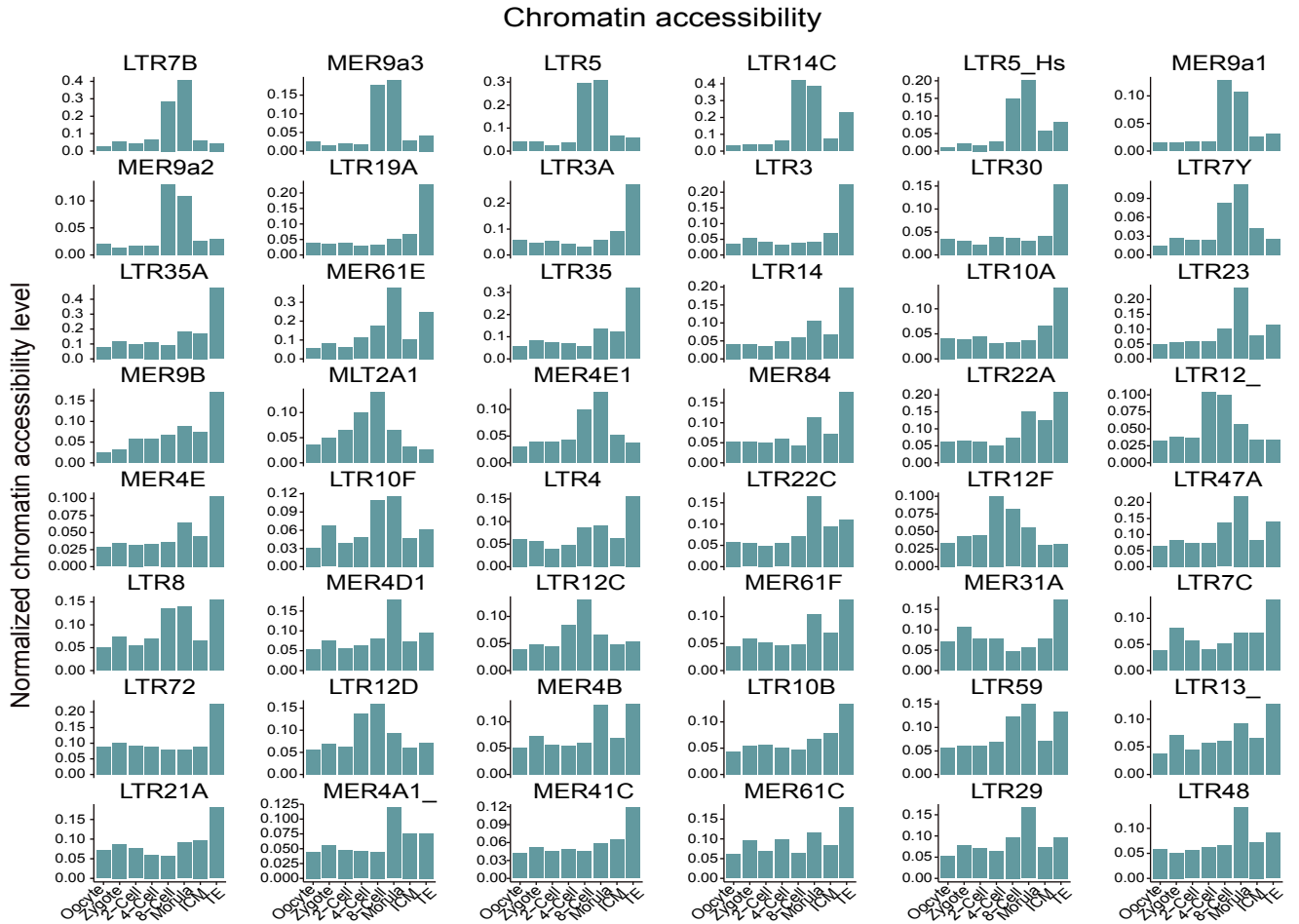
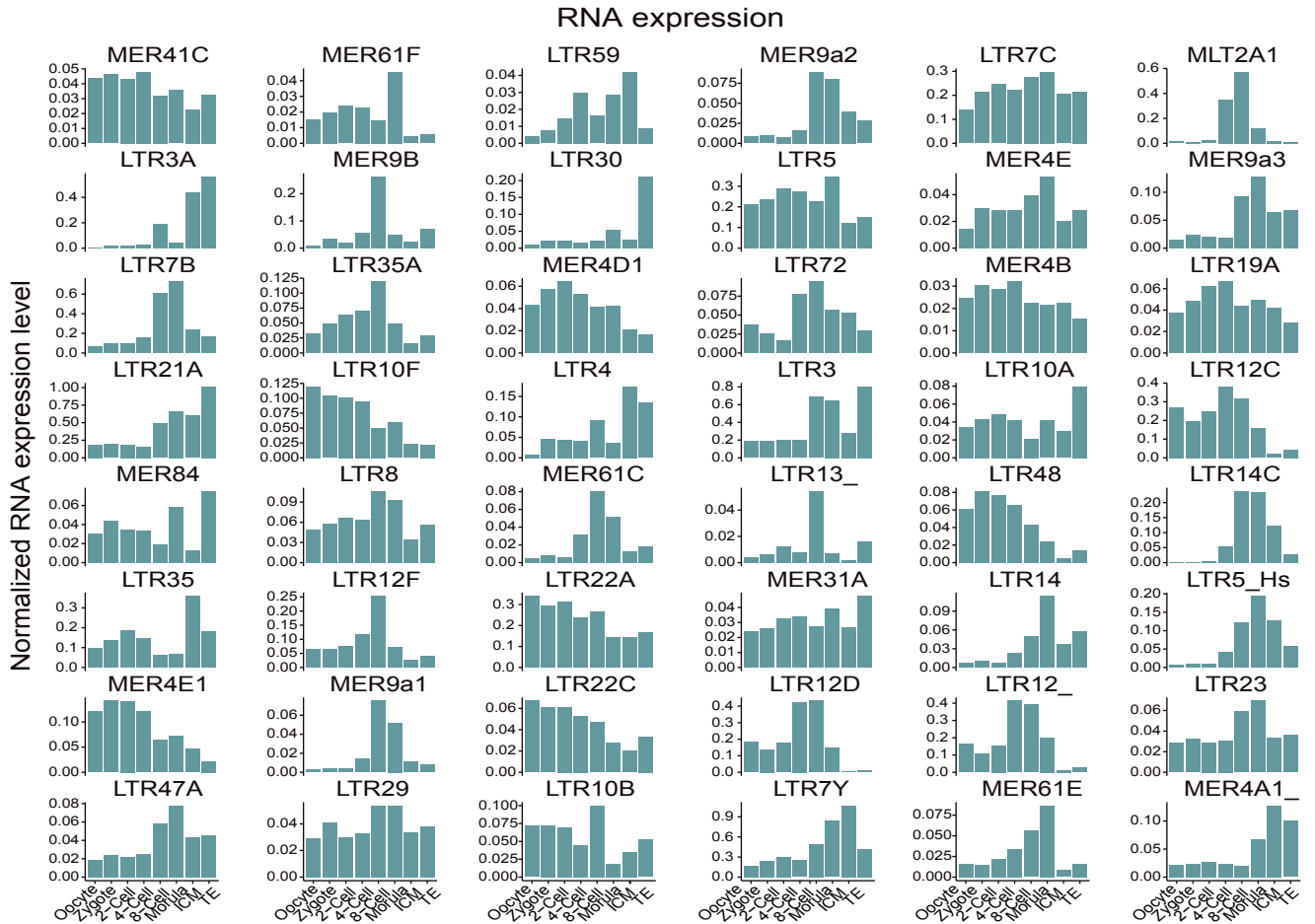




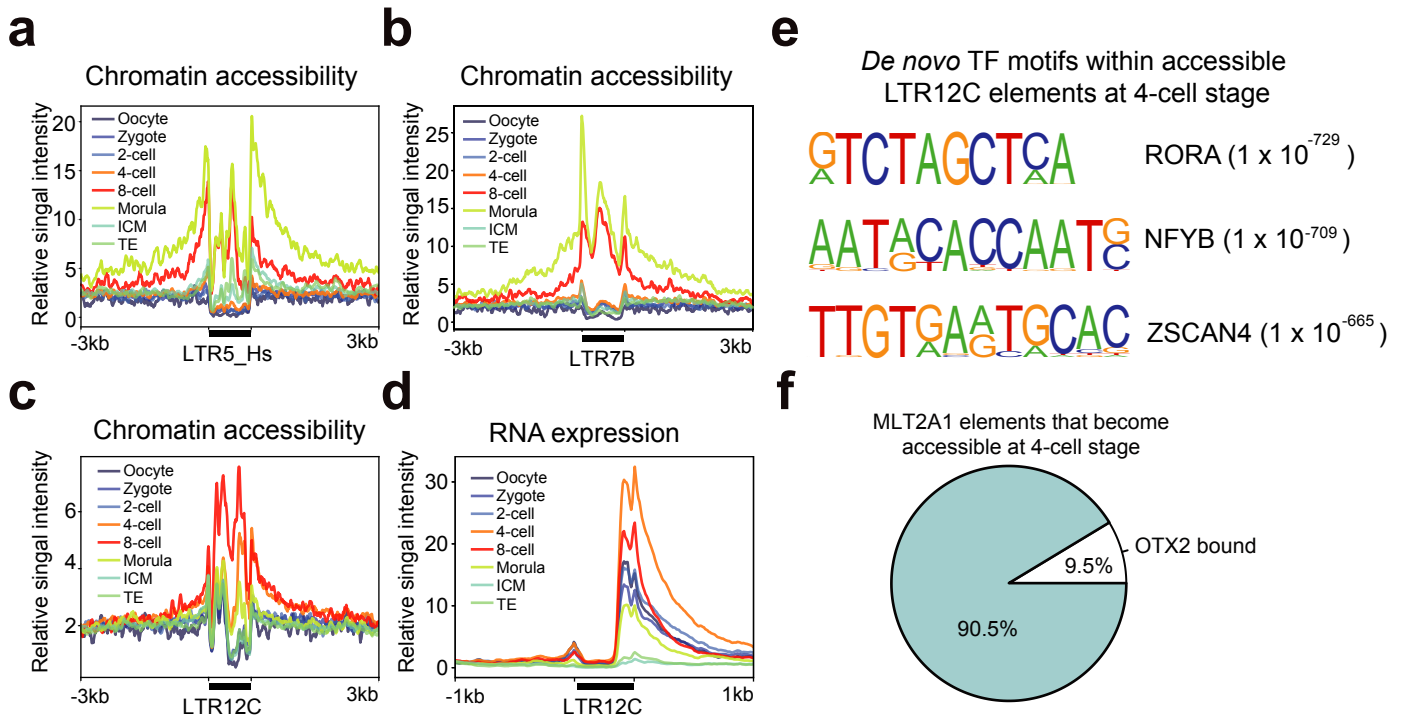
**Supplementary Figure 5: Dynamics of chromatin accessibility and gene expression during embryonic genome activation.** **(a)** Fuzzy clustering analysis of chromatin accessibility signals for the indicated stages. The individual grey lines represent the accessibility level of individual regions, and the green line represents the value for the cluster center. **(b)** The distribution of distances to the nearest TSS for regions in each cluster in **(a)**. **(c)** Mean standardized gene expression for all putative target genes for regions in each cluster in **(a)**. **(d)** and **(e)** The dynamics of gene expression **(d)** and chromatin accessibility **(e)** for representative genes in each cluster in Fig. 2a. **(f)** The dynamics of gene expression (top) and chromatin accessibility (bottom) for the indicated genes. The error bars shown in this figure represent the mean  $\pm$  standard deviation (SD) of two replicates.



**Supplementary Figure 6: DUX4 is an early regulator during embryonic genome activation.** (a) Number of gained and lost chromatin accessibility peaks at the indicated stages. (b) Heat maps showing the chromatin accessibility read enrichment on the gained accessible regions at the indicated stages. (c) *DUX4* gene expression level at the indicated stages. (d) Venn plot showing the overlap between *DUX4* binding sites and accessible regions that are gained at the 2-cell and 4-cell stages. (e) Upper panel: heat maps showing the chromatin accessibility level at the indicated stages on *DUX4* binding regions that are accessible at 2-cell and 4-cell stages. Bottom panel: heat maps showing the gene expression level of the putative target genes of *DUX4* at the indicated stages. (f) The dynamics of chromatin accessibility and gene expression for the representative genes in each category. The error bars shown in this figure represent the mean  $\pm$  standard deviation (SD) of two replicates.

**a****b**

**Supplementary Figure 7: Chromatin accessibility and expression dynamics of endogenous retroviral elements during human preimplantation development. (a)** Chromatin accessibility level of the indicated ERV elements at the indicated stages. **(b)** RNA expression level of the indicated ERV elements at the indicated stages.



**Supplementary Figure 8: Chromatin accessibility, RNA expression, and TF enrichment analysis of the key ERV elements.** (a) and (b) Chromatin accessibility read enrichment around LTR5\_Hs (a) and LTR7B (b) elements at the indicated stages. (c) and (d) Chromatin accessibility (c) and RNA (d) read enrichment around LTR12C elements at the indicated stages. (e) The enrichment of the indicated transcription factor binding motifs found within LTR12C elements that become accessible at the 4-cell stage. (f) Proportion of MLT2A1 elements that are bound by OTX2 within all MLT2A1 elements that become accessible at the 4-cell stage.

**Supplementary Table 1** Summary of the embryo and cell samples used in this study.

	Stages/Samples	Biological replicate	No. of input embryos of each replicate	No. of input cells of each replicate	Donor ID	
<b>Human</b>	MII_Oocyte	Rep.1	10 oocytes	10 cells	patient #1, #2	
		Rep.2	10 oocytes	10 cells	patient #3, #4	
	Sperm	Rep.1	15 sperms	15 cells	patient #5	
		Rep.2	15 sperms	15 cells	patient #6	
	Zygote	Rep.1	10 embryos	10 cells	patient #7, #8, #9	
		Rep.2	9 embryos	9 cells	patient #10, #11	
	2-cell	Rep.1	5 embryos	10 cells	patient #12, #13	
		Rep.2	5 embryos	10 cells	patient #15, #16	
	4-cell	Rep.1	3 embryos	12 cells	patient #17, #18	
		Rep.2	3 embryos	12 cells	patient #19	
	8-cell	Rep.1	2 embryos	15 cells	patient # 20	
		Rep.2	2 embryos	16 cells	patient #21, #22	
	Morula	Rep.1	1 embryos	17 cells	patient # 23	
		Rep.2	1 embryos	15 cells	patient # 24	
	Inner cell mass(ICM)	Rep.1	1 embryos	10 cells	patient # 25	
		Rep.2	1 embryos	9 cells	patient # 26	
	Trophectoderm cells (TE)	Rep.1	1 embryos	15 cells	patient # 25	
		Rep.2	1 embryos	14 cells	patient # 26	
	<b>Mouse</b>	4-cell	Rep.1	3 embryos	12 cells	-
			Rep.2	3 embryos	10 cells	-
Morula		Rep.1	1 embryos	13 cells	-	
		Rep.2	1 embryos	14 cells	-	
<b>hESCs</b>	hESCs-LiCAT	Rep.1	-	15 cells	-	
		Rep.2	-	15 cells	-	
	hESCs-ATAC	Rep.1	-	$\sim 5 \times 10^4$ cells	-	
		Rep.2	-	$\sim 5 \times 10^4$ cells	-	
<b>Differentiated cells</b>	Differentiated cells-LiCAT	Rep.1	-	15 cells	-	
		Rep.2	-	15 cells	-	
	Differentiated cells-ATAC	Rep.1	-	$\sim 5 \times 10^4$ cells	-	
		Rep.2	-	$\sim 5 \times 10^4$ cells	-	

**Supplementary Table 2** Primers used in this study.

---

Oligo-dT primer	5'-AAGCAGTGGTATCAACGCAGAGTACT <sub>30</sub> VN-3', where V is either A, C or G, and N is any base
Template-Switching Oligo	5'-AAGCAGTGGTATCAACGCAGAGTACATrGrG+G-3', where "r" indicates a ribonucleic acid base and "+" indicates a locked nucleic acid base
PCR primer	5'-AAGCAGTGGTATCAACGCAGAGT-3'
Transposase adapter 1	5'-TCGTCGGCAGCGTCAGATGTGTATAAGAGACAG-3'
Transposase adapter 2	5'-GTCTCGTGGGCTCGGAGATGTGTATAAGAGACAG-3'

---